

# **Droplet Ratio Deformation Model in Combination with Droplet Breakup Onset Modeling**

Adelaida Garcia-Magariño<sup>1</sup>, Suthyvann Sor<sup>2</sup>

*National Institute of Aerospace Technology (INTA), Torrejon de Ardoz, Madrid, 28850, Spain*

and

Angel Velazquez<sup>3</sup>

*Universidad Politecnica de Madrid, Madrid, Spain, 28040*

**Droplet deformation and breakup in the continuously accelerated flow field generated by an incoming airfoil have been studied. The upper limit of droplet deformation and the minimum distance to the airfoil model at which the breakup onset takes place have been modeled. Three analytical equations have been developed based on the combination of two models: a droplet deformation and trajectory model for droplets in a continuously accelerated flow field; and a breakup model for droplets in the vicinity of a leading edge of an airfoil model. The verification was made using experimental data obtained for water droplets whose diameters were in the range from 400 microns to 1800 microns impinging on airfoils of three different chord sizes moving at velocities from 50 to 90 meters per second. The rotating arm**

---

Presented as Paper 2019-3719 at the AIAA Aviation 2019 Forum, Dallas, Texas, 17–21 June 2019

<sup>1</sup>Experimental Aerodynamics, Carretera de Ajalvir, Km 4, 28850 Torrejón de Ardoz, Madrid, Spain /garciamga@inta.es.

<sup>2</sup>Head of Advanced Experimental Technique Laboratory, Experimental Aerodynamics, Carretera de Ajalvir, Km 4, 28850 Torrejón de Ardoz, Madrid, Spain/sors@inta.es.

<sup>3</sup>Aerospace Propulsion and Fluid Mechanics Department, Universidad Politecnica de Madrid, Plaza del Cardenal Cisneros 3, 28040 Madrid, Spain / angel.velazquez@upm.es.

facility at INTA was used for this purpose. The analytical equations of the model were in good agreement with the experimental data. The upper limit of droplet deformation was verified by 95.40% of the tested experimental cases and the minimum distance to the airfoil was verified in 99.65 % of the cases.

## Nomenclature

$a$	=	half maximum diameter (mm)
$a_1, a_2$	=	air velocity fitting coefficients
$a_5, a_6$	=	breakup criterion coefficients
$c_m$	=	model chord (mm)
$d$	=	horizontal distance to the airfoil (mm)
$g$	=	gravity acceleration ( $m/s^2$ )
$t_{def}$	=	characteristic deformation time (ms)
$t_{ff}$	=	characteristic flow fluid variation time (ms)
$t$	=	time (ms)
$x$	=	droplet horizontal position (mm)
$y$	=	droplet vertical position (mm)
$\alpha$	=	droplet deformation ratio
$\zeta$	=	dimensionless vertical droplet position
$\eta$	=	dimensionless horizontal droplet position
$\lambda$	=	dimensionless distance to the airfoil
$\rho_{air}$	=	air density ( $Kg/m^3$ )
$\rho_d$	=	droplet density ( $Kg/m^3$ )
$\sigma$	=	surface tension coefficient ( $N/m^2$ )
$\tau$	=	dimensionless time
$\tau_0$	=	dimensionless initial distance to the airfoil
$C_{D_{sphere}}$	=	sphere drag coefficient

- $C_{D_{disk}}$  = disk drag coefficient
- $C_p$  = coefficient of proportionality (droplet deformation model coefficient)
- $F(a)$  = dimensional droplet surface area derivative with respect to the maximum half-diameter of the distorted droplet
- $R_c$  = leading edge radius (m)
- $R_d$  = droplet radius (mm)
- $U_m$  = airfoil velocity (m/s)
- $V_{air}$  = air velocity (m/s)
- $V_x$  = droplet horizontal velocity (m/s)
- $V_s$  = slip velocity magnitude (m/s)
- $V_{sx}$  = horizontal slip velocity (m/s)
- $V_{sy}$  = vertical slip velocity (m/s)
- $We$  = Weber number
- $F(\alpha)$  = dimensionless droplet surface area derivative with respect to droplet deformation
- $\Pi_1$  = dimensionless model parameter,  $\left[ \frac{3}{8} \frac{\rho_{air}}{\rho_d} \left( \frac{R_c}{R_d} \right)^2 \right]$
- $\Pi_2$  = dimensionless model parameter,  $\frac{9 R_d}{R_c}$
- $\Pi_3$  = dimensionless model parameter,  $\frac{g R_c}{U_m^2} \left( \frac{R_c}{R_d} \right)$
- $\Pi_4$  = dimensionless model parameter,  $\frac{16}{3\pi} \frac{\sigma}{\rho_d} \left( \frac{R_c}{U_m R_d} \right)^2 \frac{1}{R_d}$
- $\mathbb{V}_{sx}$  = dimensionless horizontal slip velocity
- $\mathbb{V}_{sy}$  = dimensionless vertical slip velocity
- Subscripts**
- BK = breakup onset

## I. Introduction

Droplet aerobreakup has been widely studied over the past century, starting with the works of Lane [1], Hinze [2], Wolfe and Andersen [3], or Ranger and Nicholls [4-5], passing through Krezczkowski [6], Pilch and Erdman [7],

O'Rourke and Amsden [8], Wierzba and Takayama [9], Wierzba [10] or Hsiang and Faeth [11-12] up to more recent works of Han and Tryggvasson [13-14], Luxford et al. [15-17], Chen [18], Guildenbecher [19], Theofanous et al [20-22] or even more recently the works of Shao et al [23], Ashar et al [24], Pervukhin et al [25], Luo et al [26] and Liu [27]. A literature review is out of the scope of this article; however, the important thing to be noted here is that none of the previous works addressed the specific situation of droplets in the vicinity of airfoils, which is important, among others, in the context of supercooled large droplet (SLD) ice accretion on wing surfaces. The most similar situation is when droplets are suddenly exposed to a constant high velocity airstream. This, in fact, was applied [8] in some previous studies regarding SLD ice accretion. However, for droplets located in the leading edge vicinity of an incoming airfoil, the slip velocity increases continuously with time as opposed to a constant velocity air stream. For these unsteady conditions, little information is available in the literature. The first approach to this situation is the work of Vargas and Feo [28]. Vargas and Feo [28], in an INTA-NASA cooperation conducted an experimental study in which a rotating arm facility (where an airfoil is placed at the end of the arm) equipped with a high-speed imaging system was used to gather information on a series of water droplet global parameters as they intersected the airfoil path. Though water droplets were at ambient temperature, supercooling has appeared to have no effect on droplet deformation as concluded by Veras-Alba et al [29]. This experiment [28], that involved extensive visualization, could be considered as a first approach providing experimental insight into the phenomenon. It covered droplets diameters up to 500 microns and one airfoil chord. As a continuation, further experiments were also conducted by Vargas et al in 2011 [30] and 2012 [31] in the rotating arm facility at INTA for water droplets with diameter ranging from 500 microns to 1800 microns, airfoil velocities from 50 m/s to 90 m/s and for three airfoils chord sizes of 0.21 m, 0.47 m and 0.71 m. From the analysis of those experiments, a set of investigations were conducted [32-36]. First, in the work of Garcia-Magariño et al [32], the deformation and breakup of four droplet diameters (0.354 mm, 0.580 mm, 0.782 mm and 1.056 mm) were presented and studied. The authors concluded that the transient effects (associated to the fact that the slip velocity past the droplets continuously increased) play a relevant role. At the same time, Sor et al [33-34] developed a droplet deformation and trajectory model for droplets in the stagnation line of a moving airfoil, that proved to be considerably more accurate than previous models. Finally, two breakup criteria were proposed by the authors. First, Garcia-Magariño et al [35] developed an empirical breakup criterion that allowed to determine when breakup

takes place and second, in a very recent study, Pablo et al [36] used an instability model based on the growth of Rayleigh-Taylor waves at the droplet surface. The first of these criteria will be used in this investigation.

Recently, additional attention has been paid to the importance of unsteadiness in aerobreakup [37-39]. Kékesi et al [37] investigated numerically the unsteady deformation and breakup of an initially spherical drop in the bag and shear breakup regimes, induced by steady disturbances. They concluded that further development should be achieved by accounting for acceleration terms rather than from the investigation of stationary drops. The need of investigation of the unsteady effect of the droplets drag coefficient including the droplet deformation and internal circulation for modelling purpose is well presented by Shao et al [38], who addressed the issue numerically. They studied unsteady drag coefficient of liquid droplets by using a mass conserving level set method in the context of liquid atomization. Therefore, the droplets acceleration considered is the one of those immersed in a continuous air jet, which is a decelerating relative flow. They were only interested in droplet deformation, and therefore only Weber numbers up to 10 were considered to avoid droplet breakup. They concluded that the unsteady drag coefficient was always larger than the steady drag coefficient for the decelerating relative flow. Another interesting recent work is the one of Meng and Colonius [39] in 2017, that specifically argued in the introduction section that a definitive understanding of aerobreakup remained elusive. They studied the aerobreakup of a water droplet in the flow behind a normal wave numerically and the results suggested that the phenomenology of stripping may be better described as the simultaneous flattening and stripping of liquid material. They finally concluded that the droplet deformation alters its drag properties and unsteady effects become dominant. Unsteadiness could be even more important when instead of a constant high air streams, droplets are subjected to a continuously accelerating air stream such as in the vicinity of the leading edge of an airfoil. In this context, there is still a gap of knowledge in the underlying physics that lead to the breakup in this type of air flow (continuously accelerated). New experiments and simulations should be performed, and to this end it would be very useful to determine the conditions for the breakup.

The present article studies the breakup of droplets due to the flow field generated by an airfoil moving towards the droplet. Droplets initially deform as oblate spheroid and at some point, before the airfoil would impinge the droplet, this droplet starts the breakup under certain conditions. There are two quantities that would be very important to define new experiments to study this phenomenon: the distance to the airfoil at which droplets break up and the cross-stream diameter at that point. Increasing the distance to the airfoil at the breakup onset, the evolution of the breakup observed

would also be increased. Therefore, it would be necessary to have a minimum distance to the airfoil to study the whole phenomenon. On the other hand, previous studies such as those of Stefanitis et al [40] and Yang et al [41] seem to indicate that the cross-stream diameter of the flattened droplet at breakup onset is related with the actual breakup mode. Stefanitsis et al [40] conducted a numerical investigation of the aerodynamic breakup of Diesel and heavy fuel droplets. A parametric study was performed for the Ohnesorge number and the density ratio and their effect on the breakup mode and on various parameters such as the droplet deformation, surface area, drag coefficient and breakup initiation time was discussed. They finally concluded that the increase of Weber number resulted in an increase in the rate of the deformation of the droplets. Yang et al [41] studied the transitions of deformation to bag and to bag and stamen breakup for droplets subjected to a continuously gas flow (steady flow of air). Results indicated that the breakup modes were determined by the ratio of the cross-stream diameter of the flattened droplet to the wavelength of the most unstable Rayleigh-Taylor, being this wavelength depended only on the surface tension, droplet density and acceleration. Therefore, the droplet deformation or cross-stream diameter is an important factor that defines the droplet breakup mode.

The purpose of this investigation is to obtain simple expressions, for droplets in the vicinity of the leading edge of an airfoil, of the droplet deformation and the distance to the airfoil at the breakup onset. These simple expressions will be obtained by combining the Garcia-Magariño's droplet breakup criterion [35], which relates the Weber number at the breakup onset to the ratio of the characteristic times involves, and the Sor's droplet deformation and trajectory model [34], which consists of three dynamic equations for droplets position and deformation. Some hypotheses are assumed in order to reduce to order of the dynamic equations and simplify the problem. In particular, it is assumed that the droplet velocity and displacement are small, the air velocity behaves as a simplified analytical function and droplet breakup occurs when the droplet is deformed, which simplifies the surface area expression. These simple expressions will allow for defining experiments to study the droplet breakup in the vicinity of a leading edge of an airfoil. First, both the droplet deformation and trajectory model and the breakup criterion used are described, and the hypotheses are presented. Then, the simple expressions for maximum droplet deformation and its minimum distance to the airfoil are obtained by combining the previous models. The experimental setup is described next and the simple expressions are verified with the experimental data. Finally, results are discussed leading to the conclusions.

## II. Droplet Deformation and Trajectory Model

A droplet deformation and trajectory model for droplets in the vicinity of an airfoil was formally derived in a previous article [34]. It was assumed that the droplet deforms as an oblate spheroid and that the total volume remains constant during the deformation process. The model consists of three equations: two dynamics equations that represent the equilibrium of forces in the horizontal and vertical directions and one deformation equation. For the equilibrium of forces in the vertical and horizontal directions, the forces considered are the drag force and the gravity force. The drag force is modelled as the sum of a steady term plus an unsteady term. The steady drag force term is modelled as the interpolation between the drag of a sphere and the drag of a disk, being the interpolation coefficient dependent on the degree of deformation of the droplet. The unsteady drag force is modelled as a function of the time derivative of the slip velocity between the droplet and the air. The deformation equation represents the equilibrium of forces of half-droplet, for which the surface tension force and the pressure forces are considered. The pressure forces are assumed to be proportional to the dynamic pressure and the area, being the proportionality coefficient obtained from experimental data [42]. The variables of the equation are the horizontal and vertical position of the droplet,  $x$  and  $y$ , and the maximum half-diameter of the distorted droplet,  $a$ . The following dimensionless variables and functions are defined as follows:

$$\eta = \frac{x}{R_d}, \quad \zeta = \frac{y}{R_d}, \quad \alpha = \frac{a}{R_d}, \quad \tau = \frac{t U_m}{R_c}$$

$$\mathbb{V}_{sx} = \frac{V_{sx}}{U_m}, \quad \mathbb{V}_{sy} = \frac{V_{sy}}{U_m}, \quad \mathbb{F}(\alpha) = \frac{F(a)}{R_d}$$

where  $R_d$  is the droplet undistorted radius,  $R_c$  is the airfoil leading edge radius,  $U_m$  is the airfoil velocity,  $V_{sx}$  and  $V_{sy}$  are the horizontal and vertical component of the slip velocity between air and the droplet, and  $F(a)$  is the droplet surface area derivative respect to the maximum half-diameter of the distorted droplet. The final dimensionless equations of the model are the following, where the third equation is the one related to the deformation:

$$\frac{d^2\eta}{d\tau^2} = \Pi_1 \mathbb{V}_{sx}^2 \alpha^2 \left[ \left( C_{D_{sphere}}^{(1/\alpha)^3} \cdot C_{D_{disk}}^{1-(1/\alpha)^3} \right) + \left( \Pi_2 \frac{1}{\alpha^2 \mathbb{V}_{sx}^2} \frac{d\mathbb{V}_{sx}}{d\tau} \right) \right] \quad (1)$$

$$\frac{d^2\zeta}{d\tau^2} = -\Pi_1 \alpha^2 \mathbb{V}_{sx} \mathbb{V}_{sy} \left( C_{D_{sphere}}^{(R_d/a)^3} \cdot C_{D_{disk}}^{1-(R_d/a)^3} \right) + \Pi_3 \quad (2)$$

$$\frac{d^2\alpha}{d\tau^2} = -\Pi_4 F(\alpha) + \frac{16}{3}\Pi_1 C_P \mathbb{V}_{sx}^2 \quad (3)$$

where

$$\begin{aligned} \Pi_1 &= \left[ \frac{3}{8} \frac{\rho_{air}}{\rho_d} \left( \frac{R_c}{R_d} \right)^2 \right] \\ \Pi_2 &= \frac{9 R_d}{R_c} \\ \Pi_3 &= \frac{g R_c}{U_m^2} \left( \frac{R_c}{R_d} \right) \\ \Pi_4 &= \frac{16}{3\pi} \frac{\sigma}{\rho_d} \left( \frac{R_c}{U_m R_d} \right)^2 \frac{1}{R_d} \end{aligned}$$

The variables in previous equations are the dimensionless droplet horizontal position  $\eta$ , the dimensionless droplet vertical position  $\zeta$  and the droplet deformation  $\alpha$ , while  $\Pi_1$ ,  $\Pi_2$ ,  $\Pi_3$ , and  $\Pi_4$  are model parameters. For the definition of the model parameters,  $C_{D_{sphere}}$  stands for the drag coefficient of a sphere which depends on the Reynolds number,  $C_{D_{disk}}$  stands for the drag coefficient of the disk,  $\rho_{air}$  is the air density,  $\rho_d$  is the droplet density,  $g$  is the gravity acceleration and  $\sigma$  is the surface tension between the air and the droplet liquid. The  $\Pi_1$  parameter, which is a ratio of densities, contains information of the relative importance of the pressure forces acting on the droplet. The dimensionless  $\Pi_2$  parameter is proportional to the relation between the droplet radius and the airfoil leading edge ratio. The droplet radius determines the droplet inertial while the airfoil leading edge radius is an indication of the air acceleration. Therefore, the  $\Pi_2$  parameter contains information of the importance of the non-stationary term in the droplet drag coefficient of the model. The dimensionless  $\Pi_3$  parameter contains information of the gravity forces and finally the dimensionless  $\Pi_4$  parameter contains information of the relative importance of the surface tension forces and could be considered as a generalized form of the Weber number that includes implicitly the non-stationary terms. Note that the  $\Pi_4$  parameter is an adapted ratio of inertial to surface tension forces being inversely proportional to the Weber number multiplied by the square of the  $\Pi_2$  parameter.



### III. Droplet Breakup Criterion

Recently, a droplet breakup onset criterion was proposed by the authors for droplets in the vicinity of the leading edge of an airfoil [35]. During the deformation period, the maximum droplet diameter increases while the minimum diameter decreases. However, there is a point at which the minimum diameter stops to decrease and start to increase. From that point on, the droplet stops being an oblate spheroid and this point is the definition of the breakup onset in the criterion. The breakup criterion is based on the idea that droplet breakup should be governed by the relation between two characteristics times:

- The characteristic droplet deformation time,  $t_{def}$ , which is defined using the analogy between the droplet and the spring-mass system as follows:

$$t_{def} = \sqrt{\frac{\frac{4}{3}\pi R_d^3 \rho_d}{\sigma}}$$

- The characteristic flow field variation time,  $t_{ff}$ , which is defined as the slip velocity magnitude between the droplets and the air,  $V_s$ , divided by its time derivative:

$$t_{ff} = \frac{V_s}{\frac{dV_s}{dt}}$$

On the other hand, the breakup is assumed to be defined by the Weber number, which represents the relation between the pressure forces that tend to deform the droplet and the surface tension that opposes to the deformation:

$$We = \frac{\rho_{air} V_s^2 2R_d}{\sigma}$$

Using a large amount of experimental data (see Ref. [35]), a linear correlation was obtained between the Weber number at the breakup onset and the two characteristics times previously discussed. Finally, according to this criterion, breakup starts when the following condition is attached:

$$We = a_5 + a_6 \frac{t_{def}}{t_{ff}} \quad (4)$$

where  $a_5 = 17.53$  and  $a_6 = 17.89$ .

Eq. 4 is expressed as a function of the variables and the parameters defined in previous section II as follows:

$$\frac{256 \Pi_1}{9\pi \Pi_4} \mathbb{V}_{sx}^2 = a_5 + a_6 \frac{8}{3} \sqrt{\frac{1}{\Pi_4} \frac{1}{\mathbb{V}_{sx}} \frac{d\mathbb{V}_{sx}}{d\tau}} \quad (5)$$

In the end, this breakup criterion established a condition in the slip velocity and its derivative with time (that leads to droplet acceleration) for the breakup to start. The slip velocity also appears in the deformation equation of section II and is a function of time. If the model of section II was integrated in time, then this condition could be evaluated at each time and when it occurs it would determine the onset of breakup.

#### IV. New Combined Model

The purpose of this paper is to combine the two previous models briefly explained in sections II and III to obtain a simplified combined model that allows for the calculation of both the deformation and the distance to the model at breakup onset. First, some simplifications are made regarding the slip velocity and the droplet distance to the airfoil by assuming some hypotheses near the breakup onset. By means of these simplifications, the breakup time can be obtained directly from Eq. 5. On the other hand, Eq. 3 can be integrated and by introducing the breakup time, the deformation at the breakup onset is calculated. Distance between the droplets and the airfoil at the breakup onset could also be calculated based on the breakup time obtained and the simplifications regarding this distance.

##### A. Assumptions near breakup onset

Due to the fact that breakup onset typically occurs near the airfoil, and that the airfoil typically moves at much higher velocity than the droplet, some additional assumptions can be made in order to simplify the equations. These assumptions will be reasonable as long as indeed droplet breakup occurs near the airfoil, and the droplets velocity is small. The following assumptions were made near the breakup onset:

- The droplet horizontal velocity is considered to be small compared to the air velocity. Under this hypothesis, the slip velocity can be approximated by the air velocity:

$$(V_x)_{breakup} \ll (V_{air})_{breakup} \xrightarrow{V_s = V_{air} - V_x} (V_{sx})_{breakup} \cong (V_{air})_{breakup}$$

The slip velocity is typically less than the air velocity, and therefore this assumption implies an overestimate of the pressure load on the droplet and, consequently, an overestimate of the droplet deformation. The error of this assumption, calculated from experimental data, is less than 5%.

- The air velocity, at a first approach, is supposed to behave as  $\frac{V_{air}}{U_m} = a_1 e^{a_2 \tau}$  where  $a_1 = e^{-a_2 \tau_0}$ , which is in good concordance with the flow field in the stagnation line of an airfoil. The  $\tau_0$  value is the dimensionless time that the airfoil would take to reach the initial position, or in other words: the dimensionless initial distance to the airfoil. The value of  $a_2$  would depend on the airfoil used. It has a value of  $a_2 = 1.5$  for the experimental data obtained in this investigation.
- When the droplet is already deformed, the surface area derivative can be approximated as follows:

$$F(\alpha) = 4\pi\alpha$$

- Finally, it is assumed that the droplet horizontal displacement is small compared to the distance to the airfoil. This implies that the distance to the airfoil  $d$  is known as a function of time. If the time at which the breakup onset is obtained and the initial distance to the airfoil is known, then the distance to airfoil at the breakup onset is as follows:

$$\lambda = \frac{d}{R_c} = \tau_0 - \tau$$

Under these hypotheses, the time, the deformation and the distance to the airfoil at the onset of the breakup are obtained. The final dimensionless expressions are:

$$\tau_{BK} = \tau_0 - \frac{1}{2a_2} \ln \left( \frac{9\pi \left( a_5 \Pi_4 + \frac{8}{3} a_2 a_6 \sqrt{\Pi_4} \right)}{256 \Pi_1} \right) \quad (5)$$

$$\alpha_{BK} = \frac{3\pi}{64} \frac{c_p}{a_2^2 + \pi \Pi_4} \left( a_5 \Pi_4 + \frac{8}{3} a_2 a_6 \sqrt{\Pi_4} \right) \quad (6)$$

$$\lambda_{BK} = \frac{1}{2a_2} \ln \left( \frac{9\pi \left( a_5 \Pi_4 + \frac{8}{3} a_2 a_6 \sqrt{\Pi_4} \right)}{256 \Pi_1} \right) \quad (7)$$

The deformation at the onset of the breakup given by Eq. 6 must be an upper limit of the actual breakup found due to the fact that typically  $(V_{sx})_{breakup} \leq (V_{air})_{breakup}$ .

## V. Experimental Data

Experimental work developed in collaboration with National Aeronautics and Space Administration (NASA) yielded a large amount of data on the evolution of water droplets diameters between 400-1800 microns impinging on airfoils of three different chord sizes moving at velocities from 50 to 90 meters per seconds [30-31]. Though the results and the description of the experiments have already been published [30-32], for the sake of completeness, the experimental setup and the description of the experiments follow. Experiments were taken at the rotatory arm installation at the Instituto Nacional de Técnica Aeroespacial (INTA) in Spain. Figure 1 shows a photograph of the experimental setup. As observed in the figure, the experimental setup consisted of: the droplet generator, the rotating arm unit, the airfoil model and the acquisition system (a camera and a power illumination source). The rotating arm units consisted of an arm of length 2.2 m that rotates at velocities up to 400 rpm and at whose end each airfoil was attached. Droplets were generated by a monodispersed TSI MDG 100 and were allowed to fall in the path of an incoming airfoil. A range of droplets diameters between 400  $\mu\text{m}$  and 1800  $\mu\text{m}$  were obtained by varying the flow rate entering the generator, the orifice diameter through which the jet is emerged and the frequency at which this jet is vibrated. In order to acquire the data, a Photron SA-5 camera was used to obtain shadowgraph images at 75,000 fps, while a 2,000 W xenon lamp illuminated from the back.

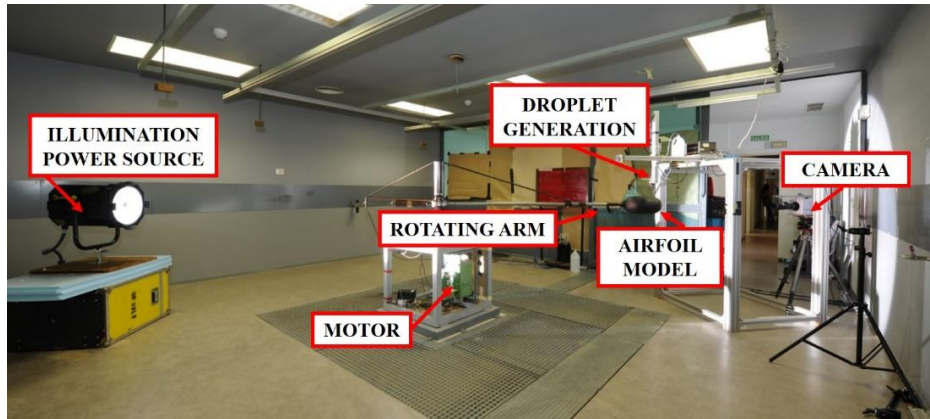


**Fig. 1 Experimental setup.**

Three airfoils models, the ones shown in Fig. 2, of the same airfoil profile and different sizes were used in the experiments. The airfoil span was the same in three cases and equal to 200 mm. The dimensionless coordinates of the airfoil profile can be seen in Table 1. A rather blunt airfoil was chosen to simulate the thickness of the commercial aircraft. Table 2 shows the dimensions of each airfoil model.

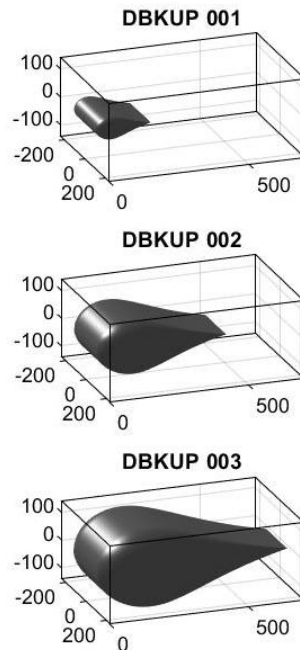


**Fig. 2 Airfoil models view.**

$X_{airfoil}/C_m$	$Z_{airfoil}/C_m$	$X_{airfoil}/C_m$	$Z_{airfoil}/C_m$
1.000	0.000	0.241	0.200
0.937	0.014	0.211	0.196

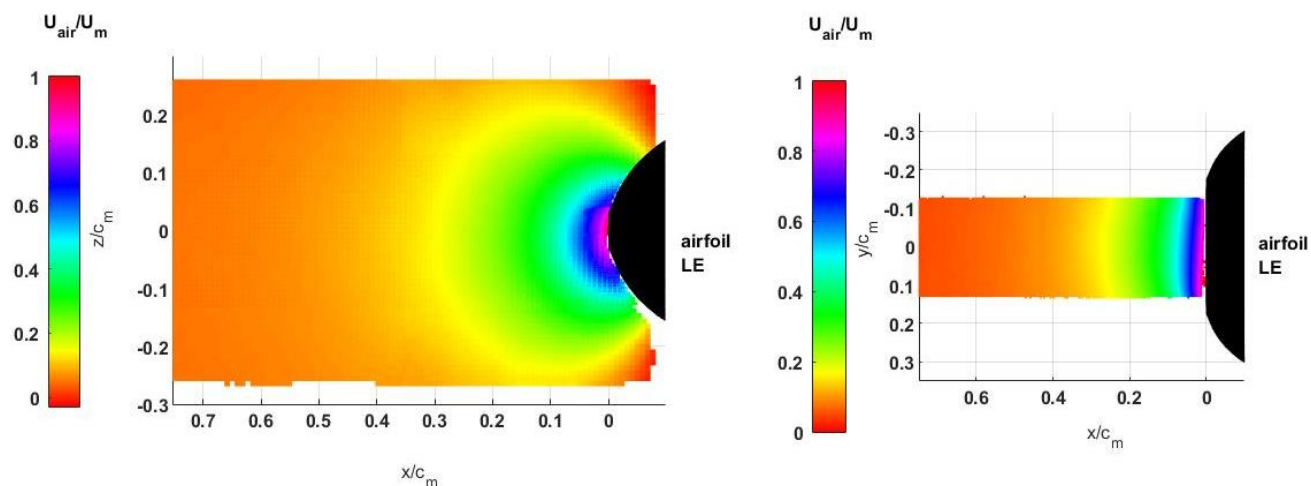
0.877	0.028	0.183	0.191
0.818	0.044	0.157	0.183
0.762	0.059	0.133	0.173
0.707	0.076	0.110	0.162
0.655	0.093	0.090	0.150
0.604	0.110	0.072	0.136
0.556	0.127	0.056	0.121
0.510	0.143	0.042	0.105
0.465	0.158	0.030	0.089
0.423	0.171	0.020	0.072
0.383	0.183	0.012	0.055
0.344	0.192	0.006	0.041
0.308	0.198	0.002	0.032
0.274	0.200	0.000	0.000

**Table. 1 Airfoil profile coordinates.**

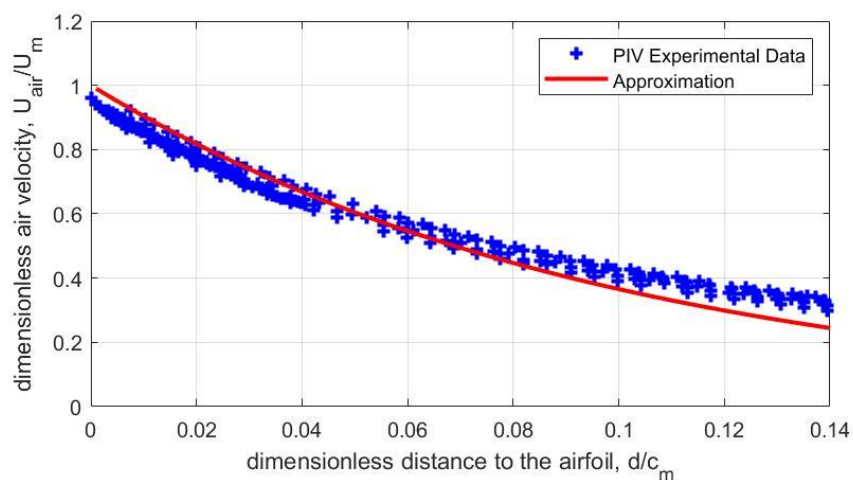
Airfoil Name	Chord, $c_m$	Rc	Thickness
DBKUP 003	690 mm	103 mm	276 mm
DBKUP 002	470 mm	70 mm	187 mm
DBKUP 001	200 mm	30 mm	80 mm

**Table. 2 Airfoil profile coordinates.**

The flow field velocity was measured in advance by means of a TSI Particle Image Velocimetry (PIV). Two pulsed Nd:Yag 190 mJ lasers were used to illuminate the flow at two consecutive instants. The time between these two pulses varied from 1.1 and 200  $\mu$ s. Each pair of images containing the two laser pulses respectively were recorded by a Power View Plus 4MP camera of resolution 2018 x 2048 pixels with different set of lenses. Olive oil particles of 1  $\mu$ m of diameters were used to seed the flow, being this olive oil particle size small enough to follow the flow. A synchronizer was used to take the pair of images at the instant at which the model is placed at a certain position in its rotation, which can be chosen in each run. Additional details of the PIV characterization of the flow field generated by these airfoils is given in the work of Garcia-Magariño [32]. The dimensionless air velocities for both the vertical and horizontal planes are shown in Fig. 3. Finally, the approximation used in this investigation for the dimensionless air flow generated by the airfoil versus the dimensionless horizontal distance to the airfoil in the stagnation line versus the experimental data obtained by the PIV is plotted in Fig. 4.



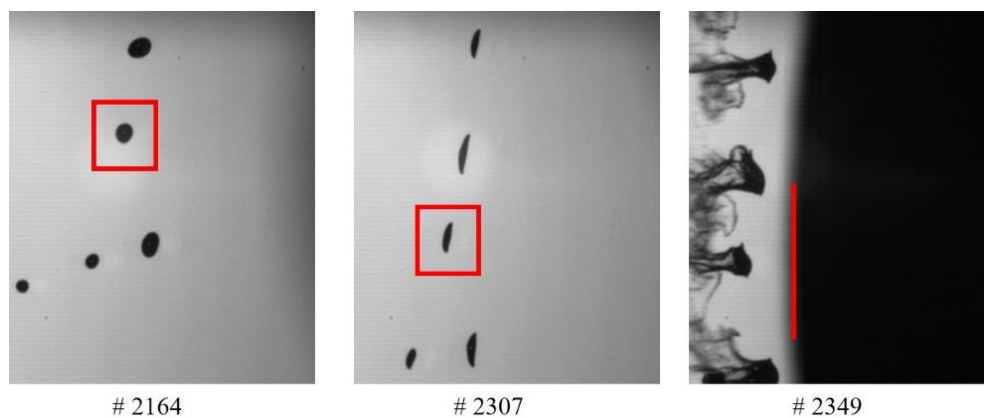
**Fig. 3 PIV dimensionless air velocity magnitude maps for the vertical plane (left) and horizontal plane (right).**



**Fig. 4 Dimensionless air velocity along the stagnation line as a function of the dimensionless distance to the airfoil.**

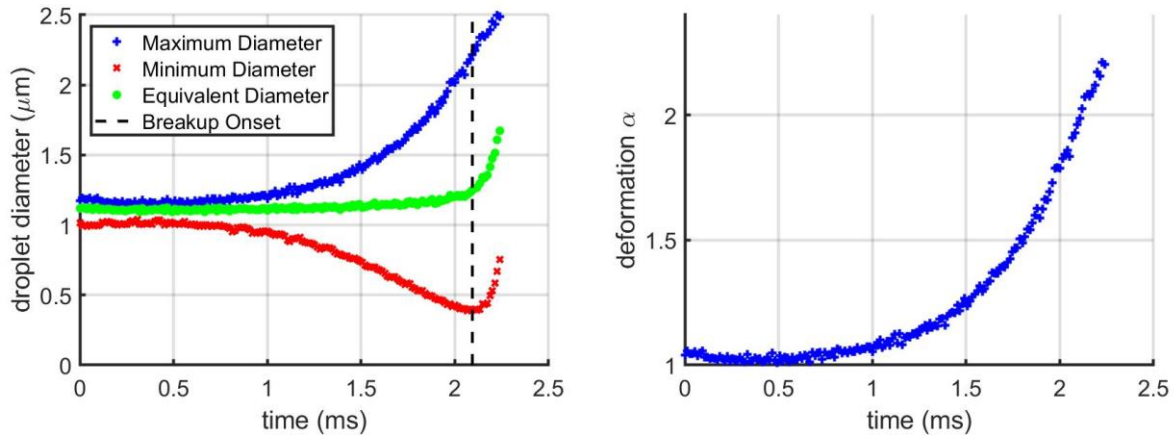
Finally, the images obtained of the droplets are analyzed to obtain the droplet trajectories and their deformation as the airfoil approached them by means of an in-house software called SITEA. An example of three frames of the images recorded used for the analysis of one droplet are shown in Fig. 5. On the left, the first frame used for the analysis can be observed. In this case, the second droplet is chosen to be analyzed and is marked by a red rectangle superimposed to the image. The middle image in Fig. 5 shows an example of an intermediate frame used for the analysis and the

image on the right corresponds to a frame where the airfoil appears in the image. First, the droplets are tracked obtaining the maximum and minimum diameter of the superimposed ellipse and its position in each frame, thus obtaining these droplets magnitudes versus time. Figure 6 on the left shows the maximum and the minimum diameter of the superimposed ellipse. As observed, the maximum diameter increases with time while the minimum diameter decreases with time up to a point where the minimum diameter stops decreasing. At this point, the minimum diameter has a minimum. Based on the assumption of an oblate spheroid, the volume of the droplet is calculated and the diameter of an equivalent sphere of the same volume is plotted in the same figure. It can be observed that the equivalent diameter remains constant up to the point where the minimum diameter has a minimum. This means that the hypothesis of an oblate spheroid is no longer valid past this point and this is used to define the breakup onset. The breakup time is thus obtained as the point at which the minimum diameter has a minimum. Figure 6 on the right shows the droplet deformation defined as the maximum diameter divided by the droplet diameter. On the other hand, Fig. 7 on the left shows the evolution of the droplet horizontal position versus time. The droplet position versus time is fitted by an exponential curve as observed in the same plot. The droplet position is derived using the prescribed fitting and the droplet horizontal velocity is shown in Fig. 7 on the right. Then, the model is detected manually when it appears in the frames recorded (see right image in Fig. 5), thus allowing for the calculation of the model position at each frame and, also, for the distance between the droplets and the airfoil versus time. Knowing this distance, the air velocity is calculated using the approximation shown in Fig. 4 and the slip velocity between the droplet and the air is calculated as the difference between the droplet velocity and the air velocity. Figure 7 on the right shows the droplet velocity, the air velocity and the slip velocity versus time.





**Fig. 5** Example of 3 images obtained from experimental tests corresponding to the analysis of one droplet.



**Fig. 6** Example of the data analysis: droplet diameter (left) and deformation (right).

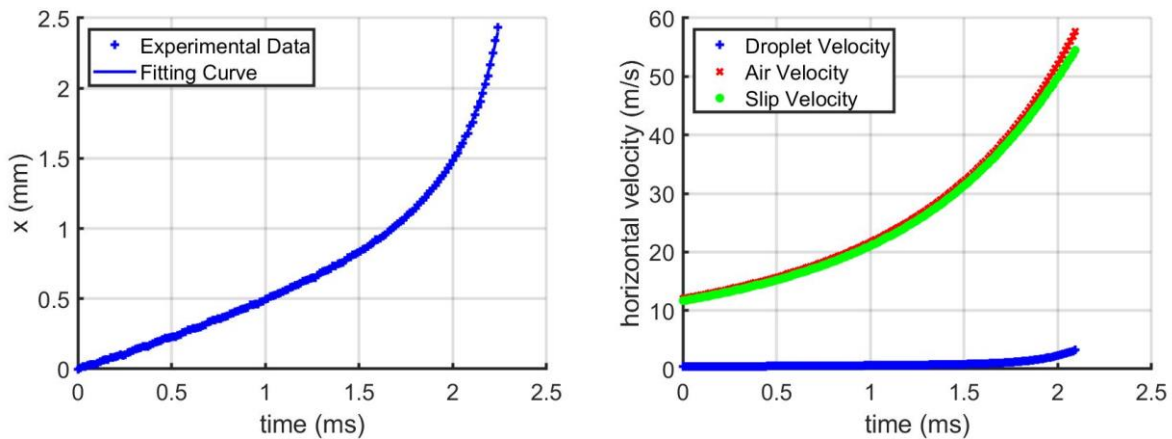


**Fig. 7** Example of the data analysis: droplet position (left) and velocity (right).

A total of 4902 droplets were analyzed including the three airfoils models, moving at five airfoil velocities of 50 m/s, 60 m/s, 70 m/s, 80 m/s and 90 m/s, and covering droplets from 400  $\mu\text{m}$  to 1800  $\mu\text{m}$  of diameter, exhibiting breakup onset a total of 1158 droplets. These experimental data were used to validate the results of the combined model.

## VI. Results and Discussion

Equation 6 provides a simple expression to calculate the droplet deformation at the breakup onset as a function of the  $\Pi_4$  parameter. Due to the hypothesis assumed, this expression would be an upper limit. Figure 8 shows the deformation of the droplets at the breakup onset obtained during the tests versus the  $\Pi_4$  parameter for all the cases tested (more than 1150 droplets), which includes droplets diameters from 400  $\mu\text{m}$  to 1800  $\mu\text{m}$ , airfoil velocities from 50 m/s to 90 m/s and airfoil chords between 200 mm and 690 mm. The  $\Pi_4$  parameter decreases with the airfoil velocity and the droplet radius and increases with the airfoil leading edge curvature. The function of Eq. 6, that provides the upper limit of the deformation of the droplets at the breakup onset, is also plotted as a solid blue line in Fig. 8.

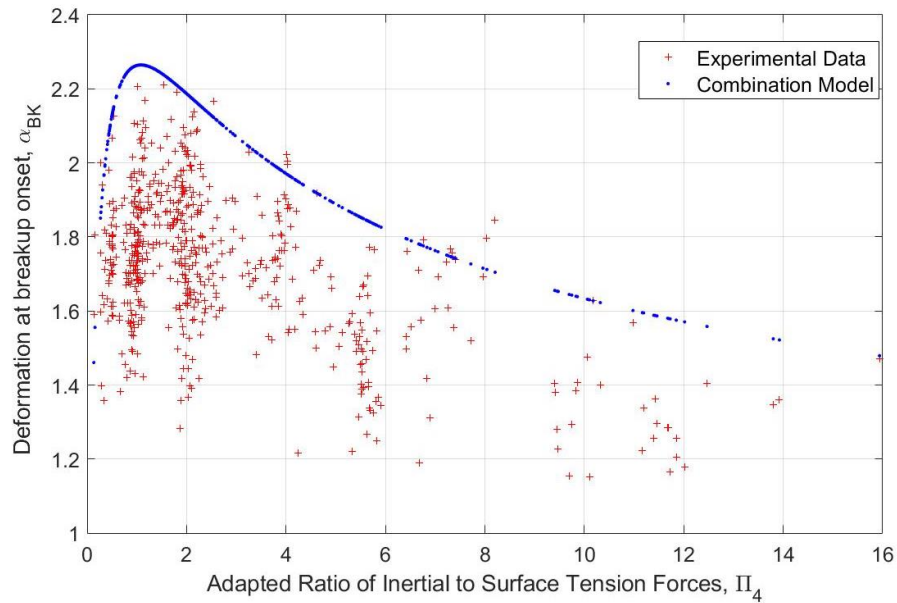


**Fig. 8. Comparisons between experimental data and droplet deformation upper limit expression of Eq. 6.**

It can be observed in Fig. 8 that the new combined model approximates an upper limit of the experimental data, as expected. The percentage of experimental cases that verifies the upper limit of deformation provided by the model was 95.40%. Also, it is observed in Fig. 8 that the deformation at the breakup onset reaches a maximum for a value of the  $\Pi_4$  parameter close to 1. This has a physical meaning. There is a relation between the  $\Pi_4$  parameter and the characteristic times of droplet deformation  $t_{def}$ , and the flow field variation  $t_{ff}$ . The characteristic deformation time is defined based on the analogy of a mass-string system and droplet deformation [8] as follows:

$$t_{def} = \sqrt{\frac{\frac{2}{3}\pi R_d^3 \rho_d}{\sigma}}$$

Following the two firsts hypotheses assumed to derive the model,  $V_s = e^{-a_2(\tau_0-\tau)}$ , the characteristic time of the flow field variation would be:

$$t_{ff} = \frac{V_s}{\frac{dV_s}{dt}} = \frac{e^{-a_2(\tau_0-\tau)}}{a_2 \frac{U_m}{R_c} e^{-a_2(\tau_0-\tau)}} = \frac{1}{a_2} \cdot \frac{R_c}{U_m}$$

Therefore the  $\Pi_4$  parameter would be:

$$\Pi_4 = \frac{16}{3\pi} \frac{\sigma}{\rho_d} \left( \frac{R_c}{U_m R_d} \right)^2 \frac{1}{R_d} = \frac{64}{9} a_2^2 \left( \frac{t_{ff}}{t_{def}} \right)^2 \quad (8)$$

For bigger droplets ( $\Pi_4$  smaller), the surface tension forces are smaller and therefore larger deformations would be expected. However, if the flow field variation times are smaller ( $\Pi_4$  smaller, see equation (8)), for bigger droplets ( $\Pi_4$  smaller), it takes more time for the droplets to notice the pressure forces and therefore the droplet deformation would be smaller. Finally, since there are two opposite tendencies, there should be a maximum as found in Fig 8. Therefore, to obtain larger deformation, the proper selection of  $\Pi_4$  parameter is required.

It is, also, important to know the minimum distance at which droplet breakup takes place as calculated by Eq. (7). First, it determines whether the breakup actually takes place, and, second, the breakup distance would be an important parameter to calculate the secondary droplets trajectories and estimate whether they will impinge or not onto the airfoil surface. Figure 9 shows the dimensionless distance between the droplets and the airfoil at breakup onset versus an adapted ratio of densities, the so-called  $\Pi_1$  parameter, and an adapted ratio of inertial to surface tension forces, the so-called  $\Pi_4$  parameter. Experimental points are displayed in the plot as red marks, corresponding to all the cases tested, which comprises droplets diameters from 400  $\mu\text{m}$  to 1800  $\mu\text{m}$ , airfoil velocities from 50 m/s to 90 m/s and airfoil chords between 200 mm and 690 mm. Also, the function provided by the combined model for the dimensionless minimum distance at which droplet breakup takes place, calculated by Eq. (7), is displayed as a surface plot. First of

all, it can be observed that almost all the experimental breakup distance points are above the minimum distance calculated by Eq. (7), as expected. The percentage of experimental cases that confirms the minimum distance to the airfoil provided by the model was 99.65%.

Secondly, only positive values of Eq. (7) have been plotted in Fig. 9. The reason is that Eq. 7 of the combined model provides an expression to determine the minimum distance between the droplets and the airfoil when droplets start to breakup. According to the combined model, droplets start to breakup at some point up to when droplets reach this minimum distance to the airfoil. However, there are cases where droplets do not breakup before impinging on the airfoil. In those cases, the airfoil intercepts the droplets before the droplets start to break. However, if we could imagine that the droplets were not intercepted by the airfoil being the airflow velocity encountered by the droplets continuously increasing with the same trend, there would be a point when droplets would start the breakup. The maximum hypothetical distance for this to happen between the droplets position and the position that the airfoil would have reached at the same time is provided by Eq. 7. The negative value given by Eq.7 would indicate that the distance is hypothetical, or in other words, the airfoil position is ahead the hypothetical droplet position. This means that droplets should breakup at some point up to where the airfoil has passed the droplets by the distance provided by Eq. 7, which means that breakup of droplets before impinging on the airfoil can be neither confirmed nor denied. On the contrary, positive distances provided by Eq. 7 mean that breakup necessarily occurs before impinging.

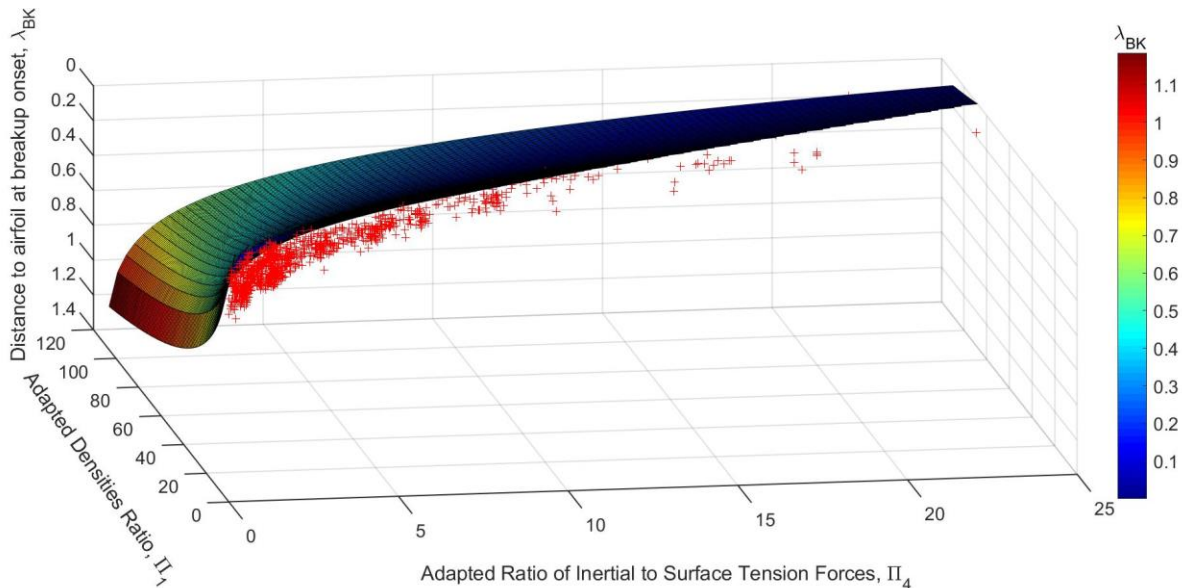


**Fig. 9: Comparisons between experimental data and droplet minimum distance to the model as given by Eq. 7.**

Finally, it can also be observed in Fig. 9 that the dimensionless minimum distance calculated by Eq. 7 is higher than 1 for some values of the parameters  $\Pi_1$  and  $\Pi_4$ , which means that for those cases breakup occurs at distances higher than the airfoil leading edge radius. This is relevant because it implies a large distance and, therefore, studies regarding the dynamics of the secondary droplets of the breakup are extremely important to calculate the catch efficiency in these cases. However, additional confirmation on this is needed since one of the assumptions was that droplet breakup occurs close to the airfoil.

## VII. Conclusions

A droplet deformation and trajectory model and a droplet breakup criterion have been combined to analyze droplet behavior in the stagnation region of a moving airfoil. The situation is relevant because the flow is unsteady in the reference frame of the droplet. In fact, in that reference frame, the flow accelerates continuously and this is the main difference with previous studies dealing with droplet deformation, dynamics, and breakup.

The combined model that has been developed, that can be summarized as a set of three simple relations, allows for the estimate of maximum droplet deformation, droplet minimum distance to the airfoil and time needed to reach breakup onset. This combined model uses four hypotheses that are reasonably met in applications that involve aircraft lifting/control surfaces when passing through rain laden regions. These hypotheses are: 1) droplet horizontal velocity is small as compared to incoming airfoil velocity; i.e.: the slip velocity can be approximated by the airflow velocity; 2) airflow velocity in the stagnation region can be approximated by an analytical function that resembles that of a “virtual” potential flow; 3) the droplet deforms as an oblate spheroid and in the limit of larger deformations, its area derivative can be approximated by the leading term of a series expansion; and 4) droplet horizontal displacement is small as to compared to the distance to the airfoil. The unsteady effects of the flow field enter the three model equations via the slip velocity and its time derivative (both time dependent). For the purpose of generalization, these two functions (time dependent velocity and its derivative) depend on the shape of the approaching body so, in principle, the model could be applied to shapes different from an airfoil. In fact, it suffices to know the functional time dependency of the incoming unsteady flow.

On the conceptual side, the model is based on a weighted comparison between the droplet characteristic deformation time (based on an analogy to a spring-mass system) and the flow variation characteristic time. This is, of

course, an ansatz type of hypothesis and it is subject to criticism. However, given the unsteady nature of the problem under consideration, it seems natural that the main governing parameters might be related to functional ratios of the characteristic times of the problem. In this context, one open question is why the model stops in the first derivative of the slip velocity. In principle, given the functional nature of the time-dependent flow generated by an incoming blunt body, higher time derivatives should be considered as well. However, experimental verification shows that the inclusion of the first derivative of the slip velocity is enough. If it is assumed that droplet breakup is related to the amplification of Taylor waves on the droplet surface caused by droplet bulk acceleration, only momentum transfer from the incoming flow to the droplet and its time variation should be considered; and this may qualitatively justify the hypotheses made. However, the authors believe that, in this frame, there are questions that still remain open and that they might be addressed in a future work.

The developed theoretical model has been verified by means of performing an experimental campaign on a rotating arm facility. Specifically, the predicted maximum droplet deformation at the breakup onset was verified by the 95 % of the experimental cases tested. Following the same trend, minimum distance to the airfoil and maximum breakup time was verified by 99 % of the experimental cases. This is surprisingly good and shows that the hypotheses used to develop the model are consistent. However, some critical questions remain open. In particular, the Weber number at the breakup onset has been related (functionally) to the ratio of droplet deformation time to flow variation characteristic time; and this functional behavior involves two coefficients ( $a_5$  and  $a_6$  in equation (4)) whose values are, basically, the same: 17.5 and 17.9 respectively. These two coefficients could be seen as fitting coefficients. So the question is why they are basically equal, and what their dependency would be on the problem parameters that have not been changed; i.e.; the types of fluids used in the experiments, and the type of time dependent fluid flow that has been considered. The authors expect to address these questions on a future work that should of a more fundamental theoretical nature.

### **Acknowledgments**

This investigation has been funded by the Ministry de Economy, Industry and Competitiveness of Spain (MINECO), as part of the project DFLOW DPI2016-75296-P. This has also been funded by INTA, under the project “Termofluidodinámica”.

## References

- [1] Lane, W. R. "Shatter of drops in stream of air." *Industrial and Engineering Chemistry*, Vol. 43, No. 6, June 1951, pp.1312-1317. <https://doi.org/10.1021/ie50498a022>
- [2] Hinze, J. O. "Fundamentals of the hydrodynamic mechanism of splitting in dispersion processes." *American Institute Chemical Engineering Journal*, Vol. 1, No. 5, Sep 1955, pp. 289–295. <https://doi.org/10.1002/aic.690010303>
- [3] Wolfe, H. E. and Andersen, W. H. "Kinetic mechanism and resultant droplet sizes of the aerodynamic breakup of liquid drops." Technical Report 0395-04 (18) SP, Aerojet General Corporation, Research and Engineering Division, 11711 Woodr. ff Avenue, Downe, California, April 1964. Prepared under D. S. Army Chemical Center Contract DA-18 108-405 CML-829.
- [4] Ranger, A. A. and Nicholls, J. A. "Aerodynamics shattering of liquid drop." *AIAA Journal*, Vol. 7, No. 2, 1969, pp. 285-290. <https://doi.org/10.2514/3.5087>.
- [5] Ranger, A. A. and Nicholls, J. A. "Atomization of liquid droplets in a convective gas stream." *International of Journal Heat and Mass Transfer*, Vol. 15, No. 6, 1972, pp. 1203–1211. [https://doi.org/10.1016/0017-9310\(72\)90185-8](https://doi.org/10.1016/0017-9310(72)90185-8)
- [6] Krzeczowski, S. A. "Measurement of liquid droplet disintegration mechanism." *International Journal of Multiphase Flow*, Vol. 6, 1980, pp. 227–229. [https://doi.org/10.1016/0301-9322\(80\)90013-0](https://doi.org/10.1016/0301-9322(80)90013-0)
- [7] Pilch, M. and Erdman, C. A. "Use of breakup time data and velocity history data to predict the maximum size of stable fragments for acceleration-induced breakup of a liquid drop." *International Journal of Multiphase Flow*, Vol. 13, No. 6, 1987, pp. 741–757.
- [8] O'Rourke, P. J. and Amsden, A. A., "The TAB method for numerical calculation of spray droplet breakup." SAE Technical Paper 872089, 1987. <https://doi.org/10.4271/872089>
- [9] Wierzba, A. and Takayama, K. "Experimental investigation of the aerodynamic breakup of liquid drops." *AIAA Journal*, Vol. 26, No. 11, May 2012, pp. 1329–1335. <https://doi.org/10.2514/3.10044>
- [10] Wierzba, A. "Deformation and breakup of liquid drops in a gas stream." *Experiments in Fluids*, Vol. 9, January 1990, pp. 59–64. <https://doi.org/10.1007/BF00575336>
- [11] Hsiang, L. P., and Faeth, G. M. "Near-limit drop deformation and secondary breakup." *International Journal of Multiphase Flow*, Vol. 18, No. 5, 1992, pp. 635–652. [https://doi.org/10.1016/0301-9322\(92\)90036-G](https://doi.org/10.1016/0301-9322(92)90036-G)
- [12] Hsiang, L. P. and Faeth, G. M. "Drop properties after secondary breakup." *International Journal Multiphase Flow*, Vol. 19, No. 5, 1993, pp. 721–735. [https://doi.org/10.1016/0301-9322\(93\)90039-W](https://doi.org/10.1016/0301-9322(93)90039-W)
- [13] Han, J. and Tryggvason, G. "Secondary of axisymmetric liquid drops. I. Acceleration by a constant body force." *Physics of Fluids*, Vol. 11, No. 12, Dec 1999, pp. 3650–3667. <https://doi.org/10.1063/1.870229>

- [14] Han, J. and Tryggvason, G. “Secondary of axisymmetric liquid drops. II. Impulsive acceleration.” *Physics of Fluids*, Vol. 13, No. 6, June 2001, pp. 1554–1565. <https://doi.org/10.1063/1.1370389>
- [15] Hammond, D.W., Luxford, G., and Ivey, P. “Role of droplet distortion and break-up in large droplet aircraft icing.” AIAA Paper 2004-411, 2004.
- [16] Luxford, G., Hammond, D.W. and Ivey, P. “Modelling, imaging and measurement of distortion, drag and break-up of aircraft-icing.” AIAA Paper 2005-71, Jan. 2005.
- [17] Luxford, G. “Experimental and Modelling Investigation of the Deformation, Drag and Break-up of Drizzle Droplets subjected to Strong Aerodynamics Forced in relation to SLD Aircraft Icing.” PhD thesis, Cranfield University, 2005.
- [18] Chen, H. “Two-dimensional simulation of stripping breakup of a water droplet.” *AIAA Journal*, Vol. 46, No. 5, May 2008, pp. 1135–1143. <https://doi.org/10.2514/1.31286>
- [19] Guildenbecher, D. R., Lopez-Rivera, C., and Sojka, P. E. “Secondary atomization.” *Experiments in Fluids*, Vol. 46, No. 3, 2009, pp. 371–402. <https://doi.org/10.1007/s00348-008-0593-2>
- [20] Theofanous, T. G., Li, G. J., and Dinh, T. N. “Aerobreakup in rarefied supersonic gas flow.” *Journal of Fluids Engineering*, Vol. 126, No. 4, 2004, pp. 516–527. <https://doi.org/10.1115/1.1777234>
- [21] Theofanous, T. G. and Li, G. J. “On the physics of aerobreakup.” *Physics of Fluids*, Vol. 20, No. 052103, 2008. <https://doi.org/10.1063/1.2907989>
- [22] Theofanous, T. G. “Aerobreakup of newtonian and viscoelastic liquids.” *Annual Review of Fluid Mechanics*, Vol. 43, Jan. 2011, pp. 661–690. <https://doi.org/10.1146/annurev-fluid-122109-160638>
- [23] Shao, C., Luo, K., Yang, Y. and Fan, J., “Direct simulation of droplet breakup in homogeneous isotropic turbulence: The effect of Weber number” *International Journal of Multiphase Flow*, Vol. 107, Oct. 2018, pp. 263-274. <https://doi.org/10.1016/j.ijmultiphaseflow.2018.06.009>
- [24] Ashar, M., Arlov, D., Carlsson, F., Innings, F. and Anderson, R., “Single droplet breakup in a rotor-stator mixer” *Chemical Engineering Science*, Vol. 181, May 2018, pp 186-198. <https://doi.org/10.1016/j.ces.2018.02.021>
- [25] Pervukhin, V. V., and Sheven, D. G. “Using of aerodynamic droplet breakup for mass-spectrometry analysis” *Talanta*, Vol. 185, August 2018, pp. 7-15. <https://doi.org/10.1016/j.talanta.2018.03.050>.
- [26] Luo, X., Huang, H., Yan, H., Yang, D., and Wang, J., “Breakup modes and criterion of droplets with surfactant under direct current electric field” *Chemical Engineering Research and Design*, Vol. 132, April 2018, pp. 882-830. <https://doi.org/10.1016/j.cherd.2018.02.033>
- [27] Liu, N., Wang, Z. Sun, M., Wang, H. and Wang, B. “Numerical simulation of liquid droplet breakup in supersonic flows” *Acta Astronautica*, 145 (2018), pp 116-130, 2018.



- [28] Vargas, M. and Feo, A. “Deformation and breakup of water droplets near an airfoil leading edge” *Journal of Aircraft*, Vol. 48, No. 5, 2011, pp. 1749–1765. <https://doi.org/10.2514/1.C031363>
- [29] Veras-Alba, B., Palacios, J., Vargas, M., Ruggeri, C. and Barkus, T. P. “Experimental Investigation of Supercooled Water Droplet Breakup near Leading Edge of Airfoil” *Journal of Aircraft*, Vol. 55, No. 5, 2018, pp. 1970-1984.
- [30] Vargas, M., Sor, S., and Garcia-Magariño, A., “Mechanism of Water droplet Breakup Near the leading Edge of an Airfoil”, AIAA Paper 2012-3129, June 2012.
- [31] Vargas, M., Sor, S., and Garcia Magariño, A., “Drag Coefficient of Water Droplets Approaching the Leading Edge of an Airfoil”, AIAA Paper 2013-3054, June 2013.
- [32] Garcia-Magariño, A., Sor, S., and Velazquez, A. “Experimental characterization of water droplet deformation and breakup in the vicinity of a moving airfoil” *Aerospace Science Technology*, 45 (2015) 490-500.
- [33] Sor, S. and Garcia-Magariño, A. “Modeling of Droplet Deformation near the Leading Edge of an Airfoil”, *Journal of Aircraft*, Vol 52, No. 6, 2015, pp 1838-1846. <https://doi.org/10.2514/1.C033086>
- [34] Sor, S., Garcia-Magariño, A., and Velazquez, A. “Model to predict water droplet trajectories in the flow past an airfoil”, *Aerospace Science and Technology*, Vol. 58, Nov. 2016, pp. 26-35. <https://doi.org/10.1016/j.ast.2016.07.015>
- [35] Garcia-Magariño, A., Sor, S., and Velazquez, A. “Droplet Breakup Criterion in Airfoils Leading Edge Vicinity” *Journal of Aircraft*, Vol. 55, No. 5 (2018), pp. 1867-1876. DOI: 10.2514/1.C034631.
- [36] Lopez-Gavilan, P., Velazquez, A., Garcia-Magariño, A. and Sor, S. “Breakup criterion for droplets exposed to the unsteady flow generated by an incoming aerodynamic surface”, *Aerospace Science and Technology* Vol 98, 2020, 105687. <https://doi.org/10.1016/j.ast.2020.105687>
- [37] Kékesi, T. Amberg, G. and Wittberg, L. P. “Droplet deformation and breakup” *International Journal of Multiphase Flow*, Vol. 66, 2014, pp. 1-10.
- [38] Shao, C. Luo, K. and Fan, J. “Detailed numerical simulation of unsteady drag coefficient of deformable droplet”, *Chemical Engineering Journal*, Vol. 308, 2017, pp. 6619-631.
- [39] Meng, J. C. and Colonius, C. “Numerical simulation of the aerobreakup of a water droplet”, *Journal of Fluid Mechanics*, Vol. 835, 2017, pp. 1108-1135.
- [40] Stefanitsis, D. Malgarinos, I., Strotos, G. Nikolopoulos, N., Karakas, E. and Gavaises, M., “Numerical Investigation of the aerodynamic breakup of Diesel and heavy fuel oil droplets” *International Journal of Heat and Fluid Flow*, Vol. 68, 2017, pp 203-215.
- [41] Yang, W., Jia, M., Che, Z., Sun, K., and Wang, W., “Transitions of deformation to bag breakup and bag to bag-stamen breakup for droplets subjected to a continuous gas flow” *International Journal of Heat and Mass Transfer*, Vol. 111, 2017, pp 884-894.

[42] Sor, S. and García-Magariño, “Modeling of Droplet Deformation Near the Leading Edge of an Airfoil” *Journal of Aircraft*  
Vol. 52, No. 6, November–December 2015, pp 1838-1846.